Experimental analysis of density fingering instability modified by precipitation

L. Binda, C. El Hasi, A. Zalts, and A. D'Onofrio

Citation: Chaos **27**, 053111 (2017); doi: 10.1063/1.4983670
View online: http://dx.doi.org/10.1063/1.4983670
View Table of Contents: http://aip.scitation.org/toc/cha/27/5
Published by the American Institute of Physics

Experimental analysis of density fingering instability modified by precipitation

L. Binda,[1,2] C. El Hasi,[2] A. Zalts,[2] and A. D'Onofrio[1]
[1]*Grupo de Medios Porosos, Facultad de Ingeniería, Universidad de Buenos Aires, Av. Paseo Colón 850, C1063ACV Ciudad Autónoma de Buenos Aires, Argentina*
[2]*Instituto de Ciencias, Universidad Nacional de General Sarmiento, Juan M. Gutiérrez 1150, B1613GSX, Los Polvorines, Provincia de Buenos Aires, Argentina*

(Received 19 December 2016; accepted 4 May 2017; published online 19 May 2017)

We analyze the effect of precipitate formation on the development of density induced hydrodynamic instabilities. In this case, the precipitate is $BaCO_3$, obtained by reaction of CO_2 with aqueous $BaCl_2$. CO_2(g) dissolution increases the local density of the aqueous phase, triggering Rayleigh–Taylor instabilities and $BaCO_3$ formation. It was observed that at first the precipitate was formed at the finger front. As the particles became bigger, they began to fall down from the front. These particles were used as tracers using PIV technique to visualize the particle streamlines and to obtain the velocity of that movement. This falling produced a downward flow that might increase the mixing zone. Contrary to expectations, it was observed that the finger length decreased, indicating that for the mixing zone development, the consumption of CO_2 to form the precipitate is more important than the downward flow. The mixing zone length was recovered by increasing the availability of the reactant (higher CO_2 partial pressure), compensating the CO_2 used for $BaCO_3$ formation. Mixing zone development rates reached constant values at shorter times when the precipitate is absent than when it is present. An analysis of the nonlinear regime with and without the precipitate is performed. *Published by AIP Publishing.* [http://dx.doi.org/10.1063/1.4983670]

Formation of precipitates is a widespread phenomenon that appears in several fields. In particular, its incidence on fingering instability might be important for geological sequestration of CO_2. Density driven instabilities are formed when a denser fluid is put on top of a less dense fluid. This triggers fingering in both, the upper and lower fluids. If the density difference is caused by a chemical reaction which produces precipitating particles, changes might be expected in the instabilities. In this article, we have studied the effect of precipitate formation on Rayleigh-Taylor instabilities analyzing the mixing zone evolution. On the other hand, the velocity of the falling particles was studied, both inside and outside the fingers in order to understand the importance of the dragging forces on the fingers. It was found that when there was precipitation, mixing zone diminished considerably. We checked that this decrease was due to the consumption of part of the reagent (CO_2, in this case) to form the solid particles instead of producing instabilities. The particle dragging force was not strong enough to compensate the reagent lack.

I. INTRODUCTION

The interest on studying the instabilities in flows caused by local differences in density lies in the wide range of related phenomena, such as reactive-diffusive systems,[1,2] transport processes, mobility of species,[3] and heterogeneities in porous media.[4–6] The understanding of dissolution-convection processes in the presence of precipitation reactions is an emerging field that is gaining in importance. In particular, the role of reactions in processes such as geological sequestration of anthropogenic CO_2 is beginning to be recognized through several CO_2 trapping mechanisms, where CO_2 dissolution and the process of forming *in situ* interstitial carbonate minerals would take place.[7] On the other hand, the buoyancy-driven instability pattern due to the density increase, brought by CO_2 dissolution itself, is an established fact in literature.[8–11]

As it is known, CO_2 is a soluble and reactive gas in water. Once it enters the aqueous phase, there is a local density increase into the gas-water interface due to the dissolution of the gas, and a temperature increase is produced by the acid-base neutralization reaction. A fingering pattern could be originated in this region, and the buoyancy-driven instability should be highly related to double-diffusive mixing, a phenomenon usually described in oceanography.[12] As CO_2 is a weak acid in water, acid-base reactions will take place producing HCO_3^- (bicarbonate anion) and CO_3^{2-} (carbonate anion), increasing the gas dissolution and acidifying the medium. The heat produced by the exothermic neutralization reactions will decrease the density of the liquid layer containing HCO_3^- at the gas-liquid interface. If the density is controlled by two variables (mass and heat) that diffuse at different rates, the layer becomes susceptible to vertical mixing and a fast acquisition of the heat of the surrounding solution takes place when falling under gravity. Heat diffuses approximately 100 times faster than solute: heat diffusion (1.4×10^{-7} m^2/s) is higher than the solutal mass diffusion (1.6×10^{-9} m^2/s). These conditions would give rise to double-diffusive mixing. On the other hand, if the aqueous phase is alkaline, we obtain a greater dissolution of CO_2 and

more CO_3^{2-} in the solution, originating more favourable conditions for the precipitation of slightly soluble carbonates such as $CaCO_3$ or $BaCO_3$. The formation of carbonates removes carbon dioxide from the liquid phase.[13,14] Such a reaction would attenuate convective motion.

Regarding deep geologic CO_2 sequestration, instabilities can be expected[15,16] when CO_2 is injected into depleted oil wells or deep saline aquifers, unfit as drinking water sources. It is important to understand this phenomenon for geological storage of this gas, taking into account that instabilities may affect the dissolution rate and long term sequestration. Many articles have been published on experimental and theoretical aspects of geological sequestration of CO_2.[17,18] The effect of temperature, CO_2 pressure, and different salt concentrations have been theoretically[19] and experimentally analysed.[20] On the other hand, the previous studies underline the interest on precipitation reactions during flow displacements in porous media in CO_2 sequestration experiences.[21–24] Mineralization yielding carbonates is a promising process for a permanent safe storage of CO_2 in different geological strata. Therefore, understanding the precipitation effects on the stability of CO_2 diffusion is particularly important.[25,26] Nagatsu *et al.*[25] reported studies on precipitation reactions in a horizontal Hele Shaw cell. $CaCO_3$ formation in porous media by *in situ* generation of reactants was reported by Redden *et al.*[27] In complex natural and engineered systems, the relative importance of individual sub-processes cannot be fully assessed without considering them as part of dynamic processes at work, where individual time and space-dependent processes are fully linked.[28] In this sense, solid phase growth and precipitation phenomena are related to different physical processes, in disciplines as diverse as atmospheric aerosol transport,[29] mineral formation in soils and other porous media,[30] transport and deposition mechanisms of nanoparticles,[31,32] formation and inhibition of scale deposition in industrial or domestic equipment[33] or geological CO_2 sequestration,[34] among others. The goal of this work is to analyze the interplay of this instability with the formation of precipitate undergoing gravitational sedimentation.

By injecting CO_2 in a porous medium or Hele-Shaw cell, the gas dissolves in the aqueous phase, which becomes denser, triggering an instability pattern. As CO_2 reacts with water, its solubility will depend on the chemical equilibria between the species

$$CO_{2(g)} \rightleftarrows CO_{2(aq)}, \tag{1}$$

$$CO_{2(aq)} + H_2O \rightleftarrows HCO^-_{3(aq)} + H^+_{(aq)}, \tag{2}$$

$$HCO^-_{3(aq)} \rightleftarrows CO^{2-}_{3(aq)} + H^+_{(aq)}. \tag{3}$$

If the aqueous phase is a solution containing $BaCl_2$ and NaOH we obtain $BaCO_3$ (solid) which precipitates according to the following equation:

$$BaCl_{2(aq)} + CO_{2(aq)} + 2\,NaOH_{(aq)} \rightleftarrows BaCO_{3(s)} + 2\,NaCl_{(aq)} + H_2O. \tag{4}$$

Among the different techniques to visualize acid-base related instabilities, the use of a colour indicator is a well known tool to obtain images to analyze. Despite that there is a reaction between CO_2 and the colour indicator, CO_2 consumption is negligible due to the low indicator concentration.

In the previous works[20,35–37] we have studied, both experimentally and numerically, fronts of the acid-base instabilities when an aqueous solution of a strong acid was put above a denser aqueous solution. In this work, the strong acid was replaced by CO_2, a weak acid that can give rise to the precipitation of carbonates. The development of instabilities was studied in different conditions, with and without precipitate, to determine the effect that these particles generate in the system. Also, using the PIV (Particle Image Velocimetry) technique, the streamlines traced by the precipitate were displayed to determine the effect of the particle flow.

II. EXPERIMENTAL

The experimental setup consists of a vertically oriented Hele-Shaw cell specially designed to work with gases at different pressures. The cell was built with two 12 mm thick, 10 cm diameter acrylic plates with a 1 mm gap obtained with a spacer. The cell has four inlets, with different valves to allow the injection of rinsing and working solutions, as well as purging with N_2 or filling with CO_2 at a desired pressure. In each experiment, to observe the effects of CO_2 dissolution, a constant CO_2 pressure is held in contact with the aqueous solution contained in the lower half of the cell. For avoiding a premature reaction of CO_2 with the solution during the injection of the aqueous phase, the cell is previously purged and loaded with N_2, and then, the solution is injected with a syringe. Once the solution is in place, we replace N_2 by CO_2 to start the experiment.[20] We use Bromocresol Green (BCG) sodium salt as a colour indicator to visualize the instabilities produced by CO_2 dissolution. As it was shown in previous works,[38] Bromocresol Green (BCG) sodium salt is a suitable pH indicator to observe this kind of instabilities. The experimental data obtained with this indicator match those observed by Schlieren technique.[38] When studying pressure induced changes in the instabilities, it was checked that concentration changes of the indicator do not substantially alter the development of the instabilities.[20] All experiments were done at room temperature (22 °C).

The correct illumination of the cell is crucial to visualize the acid base and precipitate formation reactions with the greatest possible contrast. To visualize the colour changes due to pH indicator we use white background and back light, but to visualize the precipitate, a black background and overhead lights are employed. For observing both phenomena simultaneously in the same experiment, black background for half of the cell and white background for the other half are used (Fig. 1). The experiments were recorded with a digital camera (3072 × 2304 pixels). Images, obtained every 2 s, were stored and analyzed splitting in RGB (Red, Green, Blue channels), choosing the channel with the highest black-white contrast. The mixing zone is defined as the region parallel to the interface where the concentration of the acidic solution lies between 5% and 95% either with or without precipitate. We estimate this concentration as the average length

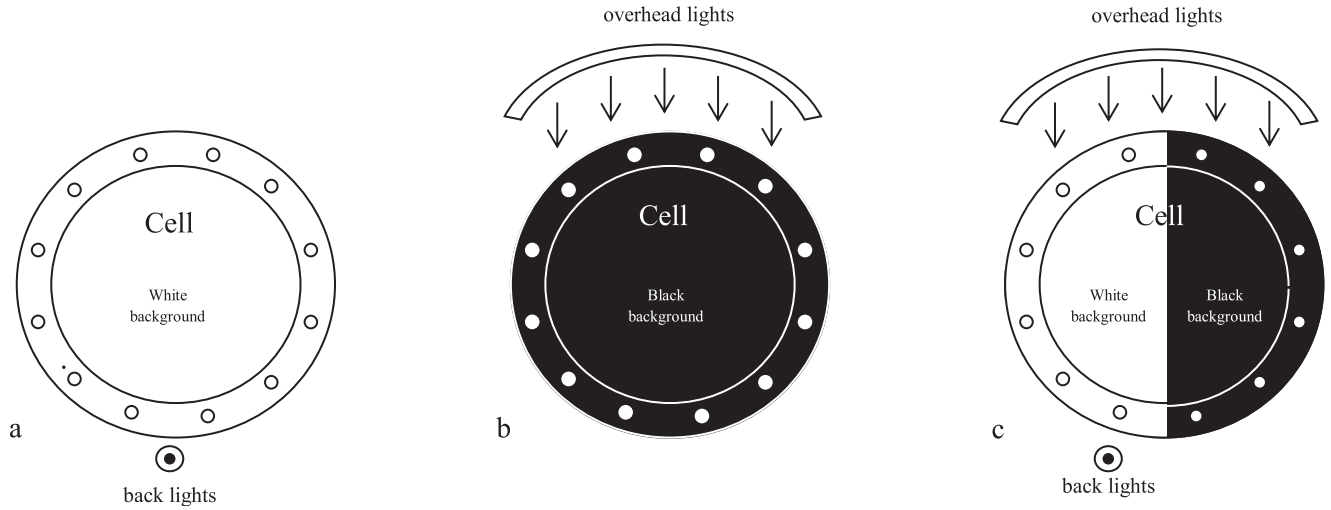

FIG. 1. Illumination set up (for more experimental details see Outeda *et al.*[20]) (a) Visualization through colour indicator changes: back lighting and white background; (b) precipitate visualization: black background and upper lighting. (c) Combination of both systems, for simultaneous visualization of precipitate formation and pH indicator.

of the fingers taking this length as the distance between the lower and upper end. This procedure is employed to determine the length of the mixing zone as a function of time.

III. RESULTS

In this paper, we examine the instabilities driven by the dissolution of CO_2 (at a fixed pressure) in an alkaline solution containing $BaCl_2$. Figure 2 (supplementary material, video) shows the development of instabilities visualized by the formation of precipitate of $BaCO_3$ at various times (acid–base reactions are taking place, but as there is no colour indicator, the effect on the pH is not observable). As the gas dissolves, it increases the local density at the interface, triggering the instabilities and reacting with the components of the solution. When $BaCl_2$ was present, the formation of a thin layer of precipitate was seen at the interface. The precipitate particles can be used as tracers. During the early development of the instabilities, the particles of precipitate follow the fingering pattern, taking the shape of the fingering front. As time evolved, many particles grow and fall down freely, creating convective precipitate currents.

On the other hand, Fig. 3(a) shows fingering by density difference, observed using a pH indicator, when CO_2 is injected into the cell containing no $BaCl_2$ (without formation of a precipitate). Figure 3(b) shows a combination of both visualization techniques used in the same experiment, to observe simultaneously the precipitate and the variation of pH. For each working condition, we performed six replicates. There were only negligible differences between the growth of the mixing zones of both visualization ways at time $t = 50$ s. The particles falling down outside the fingers were not considered. For longer times, differences are clearly observable: the mixing zone with precipitate production decreases compared to the experiment without $BaCl_2$. A complete temporal evolution of the mixing zone is shown in Fig. 4. The differences in behaviour become significant at $t = 70$ s; at $t = 150$ s,

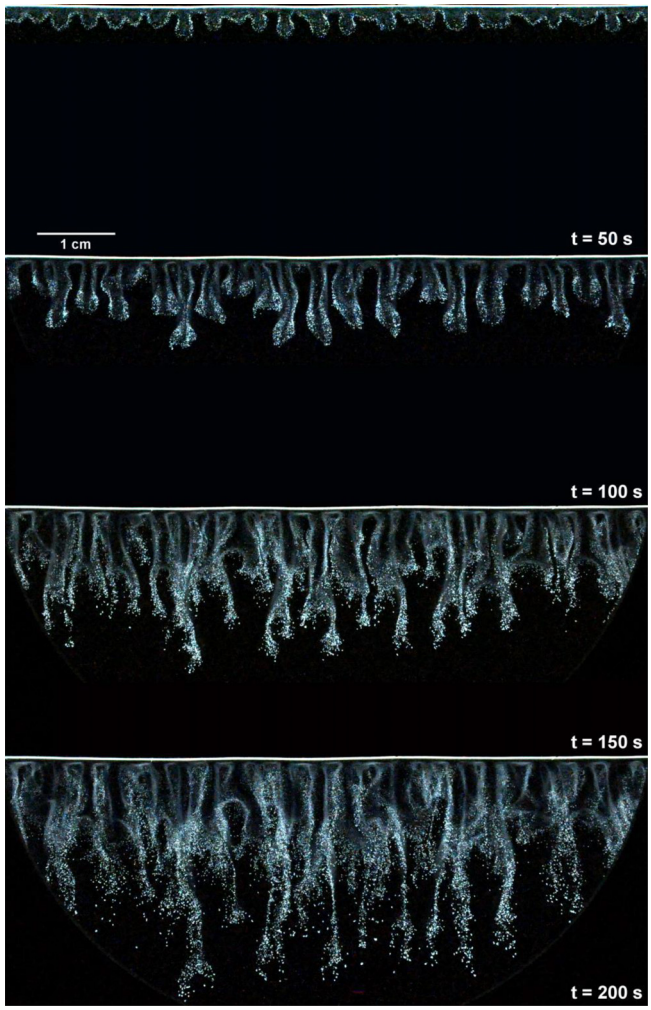

FIG. 2. Development of instabilities at $t = 50$ s, $t = 100$ s, and $t = 150$ s, caused by CO_2 (g) dissolution at 2.5 atm in an aqueous solution containing NaOH (0.01 M) and $BaCl_2$ (0.01 M).White particles are solid $BaCO_3$ (see supplementary material, video).

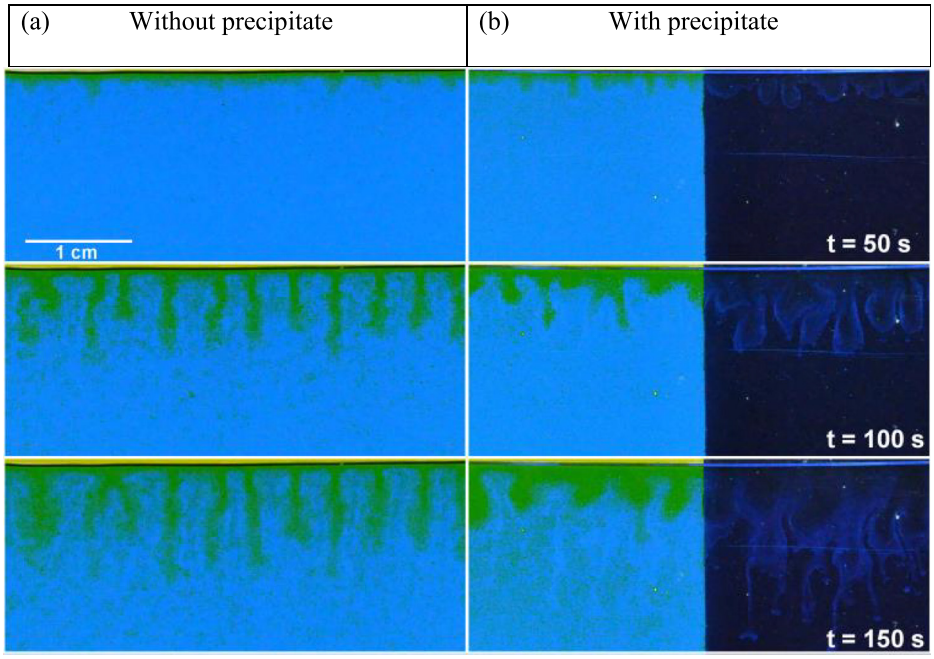

FIG. 3. Development of density driven instabilities at t = 50 s, t = 100 s and t = 150 s, induced by CO_2 (g) dissolution at 2.5 atm in an aqueous solution. (a) pH changes observed using BCG (3.2×10^{-4} M) in NaOH 0.01 M; an d(b) simultaneous visualization of pH changes and $BaCO_3$ precipitation (BCG 3.2×10^{-4} M, NaOH 0.01 M and $BaCl_2$ 0.01 M).

the mixing zone in the experiment where $BaCO_3$ was formed was about 65% of that of the non perturbed system.

Figure 3(b) shows that initially, the pattern of the precipitate matches the shape of the colour indicator changes. As the particles grow in size and number, their falling velocity exceeds the fingering growth, and convective currents appear inwards to the bulk of the solution. These convective currents are shown in Fig. 5(a), where the PIV technique is applied to the precipitate particles as tracers, to obtain their velocities and streamlines in order to describe the convective motion into the cell. On the other hand, these particles are initially formed in the contour of the fingers, where the acid base reaction was taking place, describing the streamlines within them. As the particles grew in volume, a point is reached that caused them to fall faster than the downward movement of the finger in which they were originated. This situation creates streamlines in the middle and sides of the fingers. These flows are shown in Fig. 5(b). The velocity field given in Fig. 5 matches the numerical results reported by Pau *et al.*[39]

By using PIV technique, it was determined that the average velocity of the particles, once they leave the fingers, is $81 \pm 10\ \mu$m/s, while the average velocity of the particles that were inside them is $47 \pm 10\ \mu$m/s. The average velocity of particles following the instability front (fingers) matches that obtained from the mixing zone development shown in Fig. 4 ($50 \pm 8\ \mu$m/s). This velocity was calculated taking into account the data between t = 40 s and t = 80 s, where the behavior was approximately linear.

The neutralization reaction is exothermic, so we can define thermal Peclet number $Pe_T = Lv/D_T$, where L is the Hele Shaw cell width (1 mm), D_T is the thermal diffusion

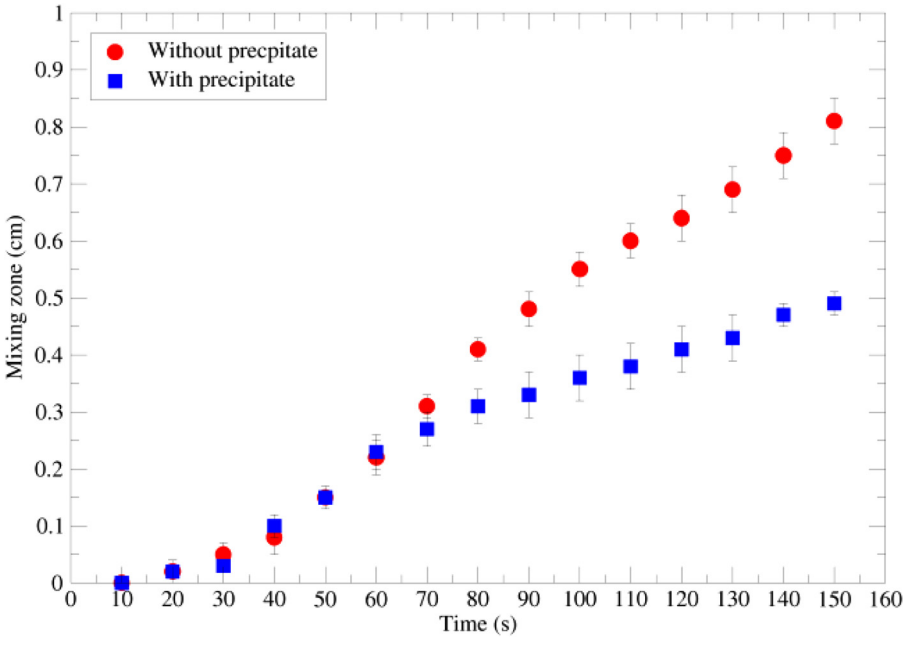

FIG. 4. Temporal evolution of the mixing zone caused by CO_2 (g) dissolution at 2.5 atm in aqueous solutions containing: ● BCG (3.2×10^{-4} M) and NaOH (0.01 M); ■ BCG (3.2×10^{-4} M), NaOH (0.01 M) and $BaCl_2$ (0.01 M). Each point is the average of 6 replicas.

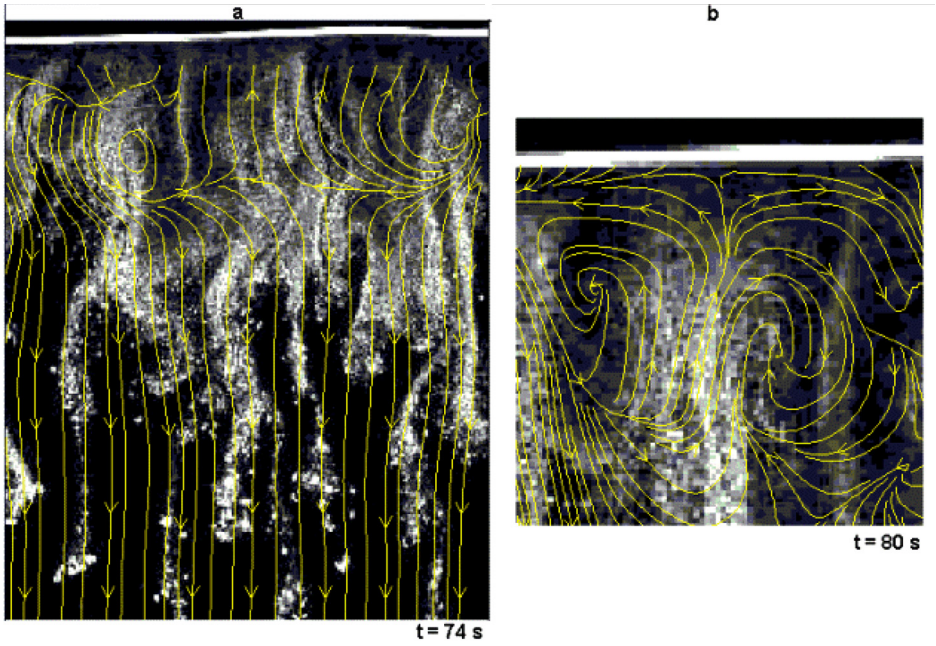

FIG. 5. (a) PIV visualization of streamlines (yellow version online) using $BaCO_3$ particles as tracers. Precipitate was produced by CO_2 dissolution in a NaOH 0.01 M and $BaCl_2$ 0.01 M solution at t = 74 s (view field is 0.73 cm × 0.59 cm). (b) Detail of movement pattern of the particles (streamlines) within a finger at t = 80 s (view field is 0.27 cm × 0.27 cm).

coefficient ($1.4 \times 10^{-7} m^2/s$), and v corresponds to the mixing zone growth rate when a constant speed is reached (90 s for the experiments done at 2.5 atm, Fig. 8). This gives $Pe_T = 2.4 \times 10^{-1}$, showing that the heat exchange is faster than the advancement of the fingers. Therefore, heat exchange with the solution and through the walls of the cell does not affect the development of the instabilities. These results coincide with what was discussed by Almarcha *el al.*[36] and Kuster *et al.*,[37] where instabilities created by neutralization reactions of a strong acid with a strong base are analyzed. If on the other hand, we calculate the value of solutal Peclet number $Pe_s = Lv/D_m$, where D_m is the mass diffusion coefficient ($1.6 \times 10^{-9} m^2/s$), we obtain $Pe_s = 2.1 \times 10^1$. Based on this result, we suggest that the convective effects generated by the instability are more important than the solutal diffusion, pointing out to a negligible contribution of the diffusion mechanism to mass transport.

IV. DISCUSSION

In the previous works, it was shown that a local disturbance of an instability front could strongly modify the instability. These disturbances may be produced by changes in the permeability of the medium or the viscosity of the solution as reported by D'Onofrio *et al.*[40] and Paterson *et al.*[41] In our case, we have the evidence of a disturbance due to an additional convective motion created by the fall of the precipitate particles. Based on this evidence, the hypothesis was that the presence of these dragging forces of the particles will perturb the instabilities produced by the dissolution of CO_2, increasing the mixing zone and its growth rate as the fingers would be guided by the particles, as shown in Fig. 6. Instead, from Fig. 4 it is clear that the mixing zone decreased sharply when the precipitate was formed, contrary to previous expectations on dragging force effects. One of the possible explanations could be that when the precipitate was formed, there was less CO_2 available for developing instabilities. Previous results reported by Outeda *et al.*[20] show that mixing zone length decreases sharply when CO_2 pressure (and therefore its concentration in the aqueous phase) is diminished. In that work, it was also shown that changing the concentration of the pH indicator does not affect the mixing zone length.

In order to have more CO_2 available for the development of the instabilities and to compensate the amount used in the $BaCO_3$ formation, we performed an experiment increasing the gas pressure over 2.5 atm, which lead to an enhanced CO_2 dissolution and a higher concentration of the carbonate species in the aqueous phase. The aim was to compensate the amount of CO_2 used to produce the precipitate, recovering the mixing zone length shown in Fig. 3(a). According to the reports of Loodts *et al.*[11] and Andres and Cardoso,[42] from the point of view of the development of the

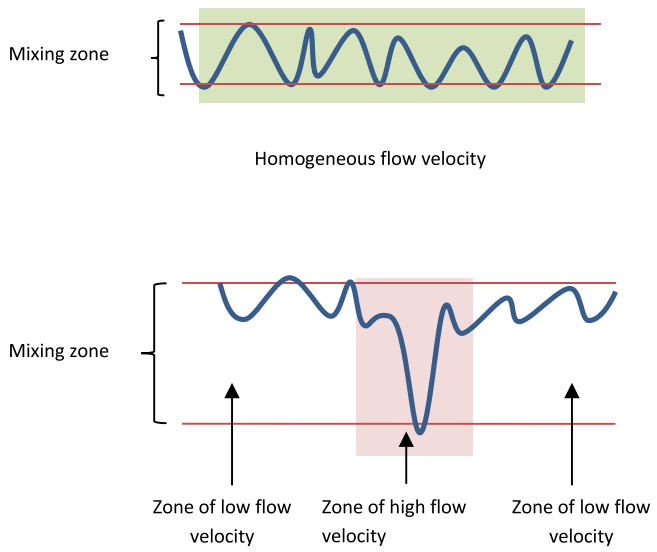

FIG. 6. Scheme of mixing zone evolution in absence and presence of zones of high flow velocity produced by perturbations of the unstable front, increase in permeability or local viscosity changes.[40,41]

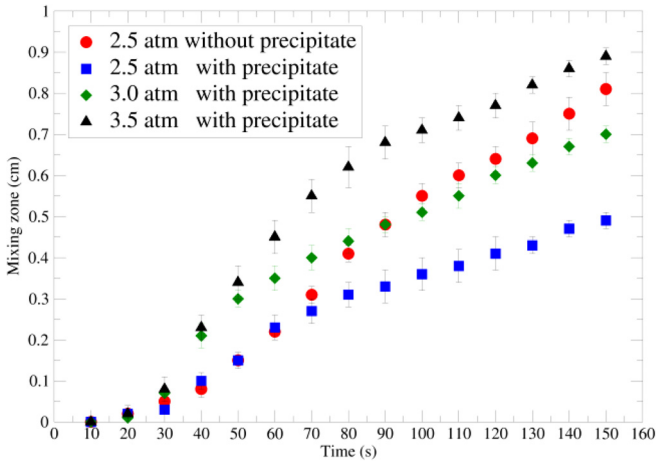

FIG. 7. Comparison of the temporal evolution of the mixing zone without formation of precipitate (red circles) with the mixing zones when $BaCO_3$ is formed at different CO_2 pressures. Data of Fig. 4 are included for better comparison of the results.

instability, a decrease of CO_2 due to the formation of a precipitate would stabilize the system. Therefore, an increase of CO_2 pressure would favor its destabilization. Figure 7 shows that the mixing zone obtained without precipitate (red circles), at 2.5 atm, and $t > 100$ s, lies between the mixing zones of the experiences made with the precipitate formation, but at 3 and 3.5 atm. This result suggests that part of the CO_2 is actually used to form the precipitate and it is not available for the development of the original instability. But, when CO_2 pressure is increased, the mixing zone develops faster and increases (from 0.5 cm to 0.9 cm for 2.5 atm and 3.5 atm, respectively, at $t = 150$ s) because more CO_2 is available.

The development rates of the mixing zones when $BaCO_3$ is formed (Fig. 8) shows that at times t between $t = 20$ s to $t = 50$ s they increase with CO_2 pressure. From about $t = 50$ s a decrease is observed until the growth rates reach approximately constant velocities at about $t = 100$ s. Note that as the pressure is increased, the system takes longer to reach this zone of constant velocity. Finally, it was clear that at $t > 100$ s, the growth rates of the mixing zone are greater in experiments without precipitate than in experiments with precipitate, independently of the increase of the pressure.

V. CONCLUSIONS

Based on previous works, it was expected that disturbances in the instability front due to falling particles would produce an increase of the mixing zone length. Nevertheless, in the particular case of the dissolution of CO_2 gas in an aqueous solution and the concomitant formation of solid particles of carbonates, the results show that the dragging force created by the falling particles does not produce an increase in the mixing zone of the instabilities. Moreover, it is observed that the mixing zone is greatly diminished by the reduction of the CO_2 available for the development of the instabilities. A large portion of the CO_2 is consumed to form the precipitate, so the remaining aqueous phase will have lower density because it will contain less solute, slowing the progress of the instability. To test this hypothesis, we found that by increasing the pressure of CO_2 when the precipitate is formed, we regain greater mixing zones. In other words, if the partial pressure of CO_2 is increased when some of the CO_2 is consumed by the precipitation reaction, the same kind of dynamics is observed as if there were no precipitate.

Therefore, in systems where instabilities occur due to the dissolution of CO_2 in an aqueous medium with experimental conditions suitable for the formation of precipitates, the finger length would decrease. An example of this case could be the fingering produced in the geological sequestration of CO_2, where the instability caused by CO_2 dissolution would tend to disappear.

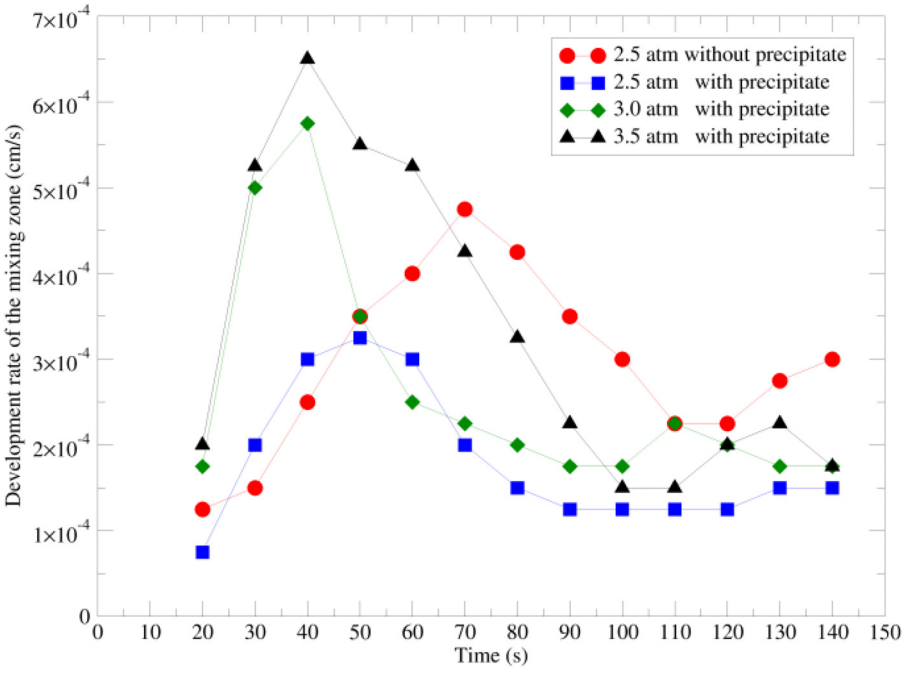

FIG. 8. Mixing zone development rates as a function of time with and without precipitate formation at different CO_2 pressures.

SUPPLEMENTARY MATERIAL

See supplementary material for movies of the experiments. The images shown here correspond to the whole Hele Shaw cell (two circular parallel plates, 10 cm diameter). 20× playback speed.

ACKNOWLEDGMENTS

Special thanks to R. Martino for the fruitful discussions about the PIV technique and ANPCyT and CONICET for financial support.

[1]J. Yang, A. D'Onofrio, S. Kalliadasis, and A. De Wit, J. Chem. Phys. **117**, 9395 (2002).
[2]I. Cherezov and S. S. S. Cardoso, Phys. Chem. Chem. Phys. **18**, 23727 (2016).
[3]G. M. Homsy, Annu. Rev. Fluid Mech. **19**, 271 (1987).
[4]L. Macias, D. Müller, and A. D'Onofrio, Phys. Rev. Lett. **102**, 094501 (2009).
[5]C. T. Tan and G. M. Homsy, Phys. Fluids A **4**, 1099 (1992).
[6]A. C. Slim, J. Fluid. Mech. **741**, 461 (2014).
[7]R. M. Dilmore, D. Allen, J. R. M. Jones, S. W. Hedges, and Y. Soong, Environ. Sci. Technol. **42**, 2760 (2008).
[8]V. Loodts, C. Thomas, L. Rongy, and A. De Wit, Phys. Rev. Lett. **113**, 114501 (2014).
[9]A. Riaz *et al.*, J. Fluid Mech. **548**, 87 (2006).
[10]M. T. Elenius and K. Johannsen, Comput. Geosci. **16**, 901 (2012).
[11]V. Loodts, L. Rogny, and A. De Wit, Phys. Chem. Chem. Phys. **17**, 29814 (2015).
[12]W. J. Merryfield, G. Holloway, and A. E. Gargett, J. Phys. Oceanogr. **29**, 1124 (1999).
[13]L. Marini, *Geological Sequestration of Carbon Dioxide: Thermodynamics, Kinetics, and Reaction Path Modeling* (Elsevier, 2007), Vol. 11.
[14]S. Bachu, W. D. Gunter, and E. H. Perkins, Energy Convers. Manage. **35**, 269 (1994).
[15]R. T. Okwen, M. T. Stewart, and J. Cunningham, Int. J, Greenhouse Gas Control **4**, 102 (2010).
[16]P. Stauffer, H. Viswanathan, R. Pawar, and G. Guthrie, Environ. Sci. Technol. **43**, 565 (2009).
[17]R. Farajzadeh, A. Barati, H. A. Delil, J. Bruining, and P. L. J. Zitha, Pet. Sci. Technol. **25**, 1493 (2007).
[18]B. Liu and Y. Zhang, Environ. Sci. Technol. **45**, 3504 (2011).
[19]V. Loodts, L. Rongy, and A. De Wit, Chaos. **24**, 043120 (2014).
[20]R. Outeda, C. El Hasi, A. D'Onofrio, and A. Zalts, Chaos **24**, 013135 (2014).
[21]J. Ennis-King and L. Paterson, Int. J. Greenhouse Gas Control **1**, 86 (2007).
[22]S. Berg and H. Ott, Int. J. Greenhouse Gas Control **11**, 188 (2012).
[23]O. Hammer, D. K. Dysthe, B. Lelu, H. Lund, P. Meakin, and B. Jamtveit, Goechim. Cosmochim. Acta **72**, 5009 (2008).
[24]C. Zhang, K. Dehoff, N. Hess, M. Oostrom, T. W. Wietsma, A. J. Valocchi, B. W. Fouke, and C. J. Werth, Environ. Sci. Technol. **44**, 7833 (2010).
[25]Y. Nagatsu, Y. Ishii, Y. Tada, and A. De Wit, Phys. Rev. Lett. **113**, 024502 (2014).
[26]P. Shukla and A. De Wit, Phys. Rev. E **93**, 023103 (2016).
[27]G. Redden, D. Fox, C. Zhang, Y. Fujita, L. Guo, and H. Huang, Environ. Sci. Technol. **48**, 542 (2014).
[28]C. I. Steefel, D. J. De Paolo, and P. C. Lichtner, Earth Planet. Sci. Lett. **240**, 539 (2005).
[29]T. M. Gaydos, R. Pinder, B. Koo, K. M. Fahey, G. Yarwood, and S. N. Pandis, Atmos. Environ. **41**, 2594 (2007).
[30]G. J. D. Kirk, A. Versteegen, K. Ritz, and A. E. Milodowski, Geochim. Cosmochim. Acta **165**, 108 (2015).
[31]W. Fan, X. H. Jiang, W. Yang, Z. Geng, M. X. Huo, Z. M. Liu, and H. Zhou, Sci. Total Environ. **511**, 509 (2015).
[32]A. E. Bayat, R. Junin, M. N. Derahman, and A. A. Samad, Chemosphere **134**, 7 (2015).
[33]D. Peronno, H. Cheap-Charpentier, O. Horner, and H. Perrot, J. Water Process Eng. **7**, 11 (2015).
[34]S. M. Amin, D. J. Weiss, and M. J. Blunt, Chem. Geol. **367**, 39 (2014).
[35]A. Zalts, C. El Hasi, D. Rubio, A. Ureña, and A. D'Onofrio, Phys. Rev. E **77**, 015304(R) (2008).
[36]C. Almarcha, P. M. J. Trevelyan, L. Riolfo, A. Zalts, C. El Hasi, A. D'Onofrio, and A. De Wit, J. Phys. Chem. Lett. **1**, 752 (2010).
[37]S. Kuster, L. A. Riolfo, A. Zalts, C. El Hasi, C. Almarcha, P. M. J. Trevelyan, A. De Wit, and A. D'Onofrio, Phys. Chem. Chem. Phys. **13**, 17295 (2011).
[38]C. Thomas, L. Lemaigre, A. Zalts, A. D'Onofrio, and A. De Wit, Int. J. Greenhouse Gas Control **42**, 525 (2015).
[39]G. S. H. Pau, J. B. Bell, K. Pruess, A. S. Almgren, M. J. Lijewski, and K. Zhang, Adv. Water Res. **33**, 443 (2010).
[40]A. D'Onofrio, V. M. Freytes, M. Rosen, C. Allain, and J. P. Hulin, Eur. Phys. J. E **7**, 251 (2002).
[41]A. Paterson, A. D'Onofrio, C. Allain, J. P. Hulin, M. Rosen, and C. Gauthier, J. Phys. France **6**, 1639 (1996).
[42]J. T. H. Andres and S. S. S. Cardoso, Chaos **22**, 037113 (2012).